Pergamon

SCIENCE DIRECT®

Tetrahedron 59 (2003) 427–431

TETRAHEDRON

Structurally isomeric two pyridino macrocycles: complexation and structures

Hiroyuki Takemura,[a,*] Noriyoshi Kon,[b,†] Mikio Yasutake[c] and Teruo Shinmyozu[c]

[a]*Department of Chemistry, Faculty of Science, Kyushu University, Ropponmatsu 4-2-1, Chuo-ku, Fukuoka 810-8560, Japan*
[b]*Department of Chemistry, Faculty of Science, Kyushu University, Hakozaki 6-10-1, Higashi-ku, Fukuoka 812-8581, Japan*
[c]*Institute for Fundamental Research of Organic Chemistry, Kyushu University, Hakozaki 6-10-1, Higashi-ku, Fukuoka 812-8581, Japan*

Received 17 September 2002; accepted 5 November 2002

This paper is dedicated to Emeritus Professor Soichi Misumi on the occasion of his 77th birthday

Abstract—Pyridine-based, structurally isomeric two macrocyclic compounds displayed a remarkably different complexation nature. The cage-type compound has an ideal structure for spherical cations, especially for the NH_4^+ ion, but the reaction with some transition metals and Ln^{3+} produced its protonated species. On the other hand, its isomer formed complexes with alkali metals and lanthanides (1:1) and also with transition metals. Some structures of the complexes were clarified by crystallographic analyses. © 2003 Elsevier Science Ltd. All rights reserved.

1. Introduction

In the previous reports, we have discussed the host–guest chemistry of the pyridine-based macrocyclic compounds **1** (Fig. 1).[1] Compound **2** is a structurally isomeric compound of **1**, which has six pyridine rings connected with four bridgehead nitrogen atoms in a different manner. Furthermore, compound **1** has rigid skeleton, but, on the other hand, compound **2** is relatively mobile compared to compound **1**. Each compound has 10 lone pairs directed to the center of the cavity. By reason of the difference in the structure, compound **1** has a suitable structure for spherical cations, but **2** has selectivity for small planar molecules such as guanidine salt and urea. Interestingly, **2** formed a complex (or hydrate) with six water molecules.[2] However, complex formation with metal cations has not been studied yet; therefore, we report herein the complexation features of **1** and **2** which result from the difference in the structures.

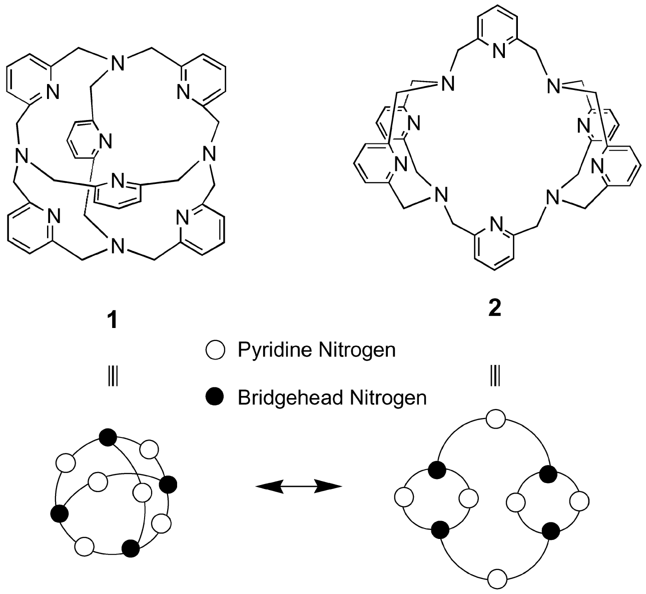

Figure 1. Structures and topologies of compounds **1** and **2**.

2. Results and discussion

2.1. Synthesis

A potassium complex of **1** was obtained from a one-pot reaction between 2,6-bis(aminomethyl)pyridine dihydrochloride and 2,6-bis(bromomethyl)pyridine under phase transfer conditions. On the other hand, compound **2** was prepared by a stepwise route via 2,11-diaza[3.3](2,6)pyridinophane.[2] Lehn et al. obtained compound **2** by the coupling reaction between 2,6-bis(bromomethyl)pyridine and 2,6-bis(aminomethyl)pyridine in the presence of a base employing acetonitrile as the solvent.[3] However, in our case, the one-step coupling reaction under phase transfer

---

Keywords: pyridinophane; cage compound; macrocyclic compound; complexation.

[*] Corresponding author. Tel./fax: +81-92-726-4755; e-mail: takemura@chem.rc.kyushu-u.ac.jp

[†] Present address: Department of Biomolecular Engineering, Graduate School of Engineering, Tohoku University, Aramaki-Aoba 07, Sendai 980-8579, Japan.

PII: S0040-4020(02)01457-6

condition (CH_2Cl_2–aq. KOH/*n*-Bu_4NBr) mainly afforded cage compound **1** and sometimes produced compound **2** as a by-product. However, we could not find a definite condition which selectively gives **1** or **2**.

2.2. Complexation study

The structural effect on the cation affinity of **1** and **2** was investigated by the observation of complex formation and stability measurements. However, several experimental difficulties limited the measurement method. The metal-free form of **1** is difficult to prepare and it is labile under aerobic conditions;[7] thus, direct observation of the reaction between **1** and M^+ is not practical. This problem was overcome by employing the competitive reaction between $M^+\subset\mathbf{1}$ and a metal salt. Previously, the stability constant of $K^+\subset\mathbf{1}$ was estimated by a competition experiment;[1b] thus, we can apply this method for estimating the stability constants of $M^+\subset\mathbf{1}$ by observing the following reaction:

$$K^+ \subset \mathbf{1} + M^+ \rightleftharpoons M^+ \subset \mathbf{1} + K^+$$

However, this reaction is very slow and more than 3 days were necessary to reach equilibrium; thus, ^{1}H NMR spectroscopy was employed. Another difficulty in the experiment is the solubility problem. We had to consider a solvent which has sufficient solubility for $K^+\subset\mathbf{1}$, **2** and also metal picrates. A desirable solvent could not be found, and thus, a two-solvent system was employed for this purpose. Because the metal complex $K^+\subset\mathbf{1}$ has low solubility in $CDCl_3$, the stability constants of $M^+\subset\mathbf{1}$ were determined in DMSO-d_6 by mixing $K^+\subset\mathbf{1}$ and metal picrates. Each aromatic signal of $M^+\subset\mathbf{1}$ appeared at a different position; thus the ratios $[K^+\subset\mathbf{1}]/[M^+\subset\mathbf{1}]$ ($M^+=Li^+\sim Cs^+$, NH_4^+) were easily obtained. Therefore, each stability constant was determined by the equations:

$$M^+ + \mathbf{1} \overset{K_1}{\rightleftharpoons} M^+ \subset \mathbf{1}: \qquad K_1 = [M^+ \subset \mathbf{1}]/[M^+][\mathbf{1}]$$

$$K^+ + \mathbf{1} \overset{K_2}{\rightleftharpoons} K^+ \subset \mathbf{1}: \qquad K_2 = [K^+ \subset \mathbf{1}]/[K^+][\mathbf{1}]$$

$$K^+ \subset \mathbf{1} + M^+ \overset{K_3}{\rightleftharpoons} M^+ \subset \mathbf{1} + K^+:$$

$$K_3 = [M^+ \subset \mathbf{1}][K^+]/[K^+ \subset \mathbf{1}][M^+]$$

$$\therefore K_1 = K_2K_3$$

On the contrary, metal-free compound **2** is readily available,[2,4] and the direct reactions between **2** and M^+ were observed by ^{1}H NMR spectra. The stability constants were measured in $CDCl_3$–CD_3CN (11/1, v/v) because compound **2** is nearly insoluble in DMSO.

As a result, $\log K=2.46$ (Na^+), 6.35 (K^+), 6.89 (Rb^+), 5.69 (Cs^+), and 6.40 (NH_4^+) were obtained in the case of $M^+\subset\mathbf{1}$, and it showed Rb^+ selectivity. The complexation of Li^+ was not observed in this method. The selectivity for the cations is relatively large, and the $\log K$ curve is steep (Fig. 2). On the other hand, the curve for that of compound **2** is gentle. K^+ selectivity was observed in this case, viz. $\log K=2.93$ (Li^+), 3.37 (Na^+), 4.62 (K^+), 2.93 (Rb^+), and 2.85 (Cs^+) were obtained. The reaction between **2** and NH_4^+ resulted in complete broadening of the signals of the host and the complex. Each signal was not separated, and thus, the stability constant could not be determined. All of the metal complexes of **1** or **2** were isolable, and 1:1 complexes were confirmed. In general, the stability of the metal complex is smaller in solvents having a large donor number than in solvents having a small donor number.[5] Therefore, the stability constants of $M^+\subset\mathbf{2}$ in DMSO should be much smaller than in the mixed solvent ($CDCl_3$–CD_3CN=11/1, v/v). Therefore, we can anticipate that the cation affinity of **1** is much larger than that of **2**. Another specific difference in the complexation properties of **1** and **2** is the exchange rate of the metal cation between the cavity and the solution. It is very slow in the case of $M^+\subset\mathbf{1}$ (>3 days) but fast in the case of **2** (immediately after mixing). Compound **1** has a spherical cavity of fixed size and is supported by a rigid skeleton. Furthermore, the cavity is surrounded by six aromatic walls. Therefore, the complexes are thermodynamically stable, and the selectivity for the cation becomes large. Also, the cation exchange rate become very slow because of the character of the cavity. On the other hand, cavity of compound **2** is easy to access from the outer environment, the molecule is very flexible compared to compound **1**; thus, the selectivity for the cation is small and the rate of complexation is fast.

Besides the alkali metal cations, complex formations with some transition metals were investigated. Preparation of the complexes was attempted by mixing $K^+\subset\mathbf{1}$ or compound **2** and the corresponding metal salts (NO_3^-, Cl^-, picrate, or

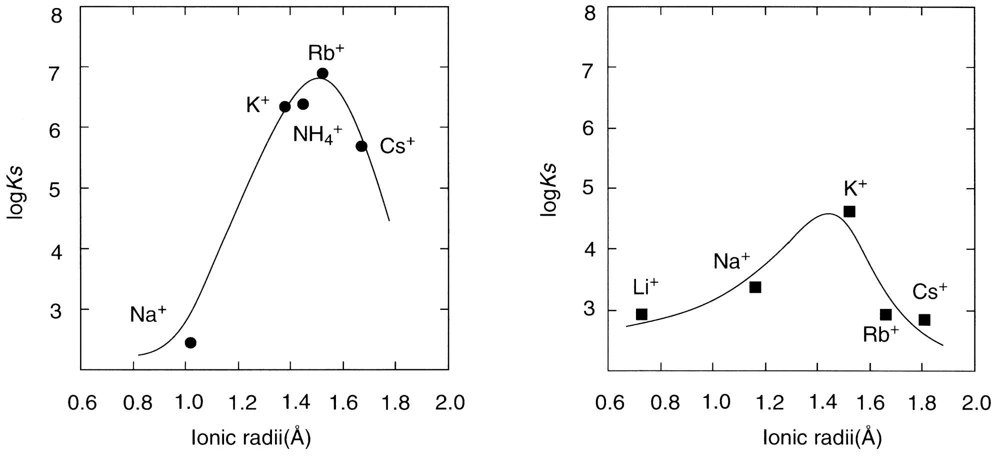

Figure 2. Plots of $\log K_s$ of $M^+\subset\mathbf{1}$, **2** vs ionic radii (Å) of the cations.

BF_4^-) in CH_2Cl_2–MeOH (1/1, v/v) or CH_2Cl_2–CH_3CN (1/1, v/v). Metal complexes (Eu^{3+}, Co^{2+}, Ag^+, and Cu^{2+}) of **2** were easily prepared and isolated, but the reaction between compound **1** and the metal salts (Eu^{3+}, Co^{2+}, Cu^{2+}, and Fe^{3+}) afforded insoluble materials, and the composition could not be identified. Alkali metal cations[6] and Eu^{3+} generate 1:1 complexes with **2**, but dinuclear complexes were obtained with Ag^+, Co^{2+}, and Cu^{2+}. The attempt to prepare Cu^+ complex of **2** failed, because the Cu^+ complex was very easy to be oxidized to Cu^{2+} complex under usual experimental conditions. The reason why alkali metal and Eu^{3+} formed 1:1 complex and other metals formed dinuclear complex is unclear so far. The coordination number of the metals and the preference of the coordination geometry seem to be concerned with these phenomena, but details are equivocal.

The transition metal complexes, $Cu^+\subset$**1**, $2Ag^+\subset$**1**, and $Ag^+\subset$**1** were easily obtained, and the properties have already been reported.[7] These are important key intermediates to synthesize metal-free **1**. However, the complexes of the transition metals, Eu^{3+}, Co^{2+}, Cu^{2+}, and Fe^{3+}, were not obtained. In the previous report, we clarified that the fluorine derivative of **1** generates protonated species with cations which have large hydrolysis constants[8] or small cations.[9]

$$xM^{n+} + yH_2O \overset{K}{\rightleftharpoons} M_x(OH)_y^{n-y} + yH^+$$

A similar principle is applicable to compound **1**, and according to this, almost all of the transition metal complexes are difficult to generate because they are too small and they have large hydrolysis constants. Furthermore, the affinity of compound **1** for protons is much larger than that of the fluorine derivative, thus the complexes could not be obtained in these metal cases.[1b,7,9] Only Tl^+ can probably generate a stable complex. Examples of the hydrolysis constants of the metal cations are as follows (x=1, y=1): $-\log K_{11}$=Li^+ (13.9), Na^+ (14.7), K^+ (14.46), Ag^+ (12.0), Eu^{3+} (7.8), Co^{2+} (9.65), Cu^{2+} (7.96), Fe^{3+} (2.19), and Tl^+ (13.3).

Despite the fact that the number of the donor units (pyridine) and the lone pairs of these two macrocyclic compounds are the same, the complexation properties are quite different. This phenomenon resulted from the difference in the topology of the molecule: spatial arrangement of the donor strongly affects the molecular properties. Therefore, we have to be careful in designing a molecule which has the desirable properties we want.

2.3. X-Ray crystallographic analyses

2.3.1. Crystal structure of $2Ag^+\subset$2. In order to confirm the coordinating structure, X-ray crystallographic analysis of $2Ag^+\subset$**2**·$2BF_4^-$ was achieved (Fig. 3). The three pyridine and two bridgehead nitrogen atoms coordinate to each Ag^+ ion in a distorted pyramidal fashion. Each pyridinophane unit of **2** is in a *syn* form, and its methylene unit is in a boat–boat conformation. This type of conformation is also observed in other transition metal complexes of 2,11-diaza[3.3](2,6)pyridinophane.[10] The Ag^+–N(bridgehead) distance is an average of 2.52 Å, and it is longer than that of Ag^+–N(pyridine) distance (average of 2.36 Å). The pyridine–Ag^+–pyridine angles in the pyridinophane units are 73.2° and 73.1°, respectively. In a previous report, we described that the Ag^+–Ag^+ distance of $2Ag^+\subset$**1** (2.78 Å) is shorter than that of metallic silver (2.89 Å) and it has a possibility of a Ag–Ag bond.[7] On the other hand, the Ag^+–Ag^+ distance of $2Ag^+\subset$**2** is much longer (4.84 Å) than that, and there is no interaction or bond between the two Ag^+ atoms. The dinuclear complex, $2Ag^+\subset$**2**, easily decomposes under light or by heating similar to other common silver complexes, and this is quite in contrast to the fact that $2Ag^+\subset$**1** and $Ag^+\subset$**1** are abnormally stable under strong light, heat, and the attack of halides (Cl^-, Br^-, I^-).[7] The $2Ag^+\subset$**2** decomposed in a day under room light, and the solution immediately turned black on heating.

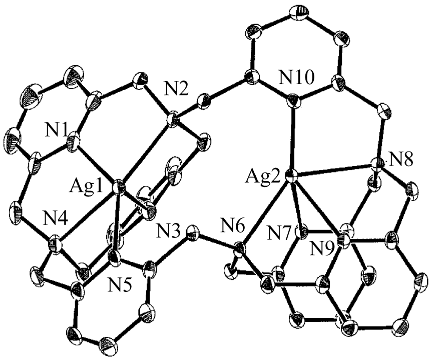

Figure 3. Molecular structure of silver complex, $2Ag^+\subset$**2** (hydrogen atoms are omitted for clarity).

2.3.2. Crystal structure of $NH_4^+\subset$1. Our interest focused on the coordination structure of $NH_4^+\subset$**1** because the host **1** has an ideal structure for the NH_4^+ complexation: especially, the geometry of NH_4^+ and its hydrogen bond pattern in the cavity of **1**. After several attempts, the structure of $NH_4^+\subset$**1** was elucidated by X-ray crystallographic analysis (Fig. 4). The molecule was disordered even at low temperatures (−150°C). The overall structure of the ligand is similar to that of $K^+\subset$**1**,[2c] and NH_4^+ is placed at the center of the cavity. The four bridgehead nitrogen atoms are directed inward, and they form hydrogen bonds with each proton of NH_4^+. The average distance of N–$H^+\cdots$N (bridgehead) is 2.38 Å, and the bond angles of N–$H^+\cdots$N (bridgehead) are

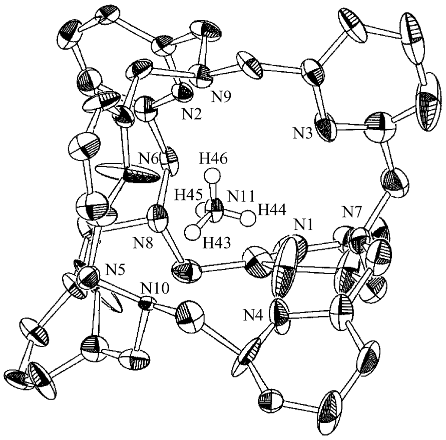

Figure 4. Crystal structure of $NH_4^+\subset$**1** (thermal ellipsoids are drawn with 50% probability).

approximately linear (169–176°). The average distance of $N^+(H)\cdots N$ (bridgehead) is 3.19 Å, which is identical to that of $N^+(H)\cdots N$ (pyridine) (3.19 Å).

The ammonium proton favors tetrahedrally arranged bridgehead nitrogen atoms rather than octahedrally arranged pyridine nitrogen atoms in spite of the identical $N^+(H)\cdots N$ distances. This is explained by the complementarity of the host–guest geometry; a tetrahedral binding site favors a tetrahedral guest, and vice versa. Furthermore, the basicity of the bridgehead nitrogen atom is somewhat larger than that of pyridine (pK_a of tribenzylamine, 4.1 in DMSO, 12.3 in nitromethane; pyridine, 3.5 in DMSO, 11.95 in nitromethane).[11] Because the benzene analog of **1** which contains only four bridgehead nitrogen atoms does not form complexes with NH_4^+,[1] the dominant factor in NH_4^+ complexation of **1** is the electrostatic interaction with the pyridine rings but not the hydrogen bonds with the bridgehead nitrogen atoms. The weak hydrogen bonds merely determine the direction of the N–H$^+$ bonds.

3. Conclusion

The topology of the host molecule greatly affected the metal complexation properties. This result provides an index for the design of the host molecule. The cage-type compound prefers spherical cations, and the protonation reaction dominates with acidic and small transition metals. On the other hand, the structural isomer which is built with [3.3](2,6)pyridinophane units binds a wide variety of guests, i.e. guanidine salt, urea, water molecules, alkali metal cations, transition metal cations, and even rare earth metal ions, although its binding ability is not very large. These definitive differences of the guest selectivity arise from the topology (spatial arrangement of the pyridine donor and the shape of the cavity) and rigidity of the molecule (the compound **1** is rigid, but **2** is more flexible).

4. Experimental

4.1. General procedures

All melting points were measured in Ar or N_2 sealed tubes and were uncorrected. ^{1}H NMR spectra were recorded at 270 MHz in $CDCl_3$ (TMS as an internal standard), CD_3OD, DMSO-d_6, and $CDCl_3/CD_3CN$ mixture (solvent signal as an internal standard). Mass spectra were recorded with *m*-NBA as a matrix.

X-Ray crystallographic analyses. Measurements were performed on a Rigaku RAXIS-IV imaging plate area detector with graphite monochromated Mo Kα radiation for $NH_4^+\subset$**1**·Pic$^-$ and on a Rigaku RAXIS-RAPID imaging plate diffractometer with graphite monochromated Mo Kα radiation for $2Ag^+\subset$**2**·$(BF_4^-)_2$. Structures were solved by direct methods (SHELXS-97[12] for $2Ag^+\subset$**2**·$(BF_4^-)_2$ and SIR92[13] for $NH_4^+\subset$**1**·Pic$^-$) and refined by full-matrix least-squares techniques.[14] The non-hydrogen atoms were refined anisotoropically. For $NH_4^+\subset$**1**·Pic$^-$, the hydrogen atoms were included, but their positions were not refined, and the isotopic *B* values were refined. All calculations were performed using the teXscan crystallographic software package from Molecular Structure Corporation.

Measurements of stability constants by ^{1}H NMR spectra. In each NMR tube, about 3 mg of $K^+\subset$**1**·Br$^-$, 4–7 mg of metal picrates, and DMSO-d_6 were weighed exactly. Initial concentrations of the host were $2.66–3.91\times10^{-3}$ mol L^{-1} and concentrations of the metal picrates were 1.62–47.9×10^{-3} mol L^{-1}. Each sample was left in a temperature-controlled water bath (25±0.1°C) for a week, and then ^{1}H NMR spectra were observed. The intensities of doublets and triplets of the pyridine rings were measured and used for calculation. In a similar way, samples of compound **2** and metal picrates were prepared. The initial concentration of the host was 3.92×10^{-3} mol L^{-1} ($CDCl_3$–CD_3CN=11/1, v/v), and the concentrations of metal picrates were 0.48–1.75×10^{-3} mol L^{-1}.

4.2. Preparation of the metal complexes

4.2.1. $2Cu^{2+}\subset$2·$4NO_3^-$·$3CH_3OH$. To a solution of compound **2** (51.4 mg, 7.5×10^{-2} mmol) in a mixed solvent (CH_2Cl_2–CH_3CN=3/2) was added a solution of $Cu(NO_3)_2\cdot3H_2O$ (64.2 mg, 2.7×10^{-1} mmol) in 1 mL of CH_3CN and the mixture then stirred at room temperature overnight. The resultant precipitates were filtered and recrystallized from CH_3OH–CH_3CN. Greenish blue prisms (11.4 mg, 13.1%). MS (FAB) *m/z* 936 (2.1%, $[M+^{63}Cu_2N_2O_6]^+$), 938 (1.6%, $[M+^{63}Cu^{65}CuN_2O_6]^+$), 940 (0.6%, $[M+^{65}Cu_2N_2O_6]^+$). Anal. calcd for $C_{42}H_{42}N_{14}O_{12}Cu_2\cdot3CH_4O$: C, 46.67; H, 4.54; N, 16.94. Found: C, 46.47; H, 4.70; N, 16.93%.

4.2.2. $Eu^{3+}\subset$2·$3ClO_4^-$·$2H_2O$. To a solution of compound **2** (53.1 mg, 7.7×10^{-2} mmol) in 3 mL of CH_2Cl_2 was added a solution of $Eu(ClO_4)_3\cdot6H_2O$ (168.8 mg, 0.3 mmol) in 5 mL of CH_3OH and the mixture then stirred at room temperature for three days. The resultant precipitates were filtered and recrystallized from dioxane-CH_3CN. White powder (63.6 mg, 59.4%). MS (FAB) *m/z* 936 (2.9%, $[M+^{151}Eu^{35}ClO_4]^+$), 938 (3.8%, $[M+^{153}Eu^{35}ClO_4]^+$, $[M+^{151}Eu^{37}ClO_4]^+$), 940 (1.2%, $[M+^{153}Eu^{37}ClO_4]^+$). Anal. calcd for $C_{42}H_{42}N_{10}O_{12}Cl_3Eu\cdot2H_2O$: C, 43.00; H, 3.95; N, 11.94; found: C, 42.76; H, 3.83; N, 11.82%.

4.2.3. $2Ag^+\subset$2·$2BF_4^-$·H_2O. A solution of **2** (49.7 mg, 7.2×10^{-2} mmol) and $AgBF_4$ (32.1 mg, 0.16 mmol) in 3 mL of CH_2Cl_2 was stirred for a day in the shade. The resultant solution was filtered through Celite and the solvent was evaporated. The powder thus obtained was rinsed with water, dried, and recrystallized from CH_3OH. Colorless needles (14.0 mg, 17.8%). Mp >271.5°C (dec. N_2 sealed tube); ^{1}H NMR (CD_3OD): δ 8.18 (t, 2H, J=7.5 Hz), 7.81 (d, 4H, J=7.0 Hz), 7.14 (t, 4H, J=7.5 Hz), 6.58 (d, 8H, J=7.0 Hz), 5.01 (s, 8H), 4.40 (d, 8H, J=14.1 Hz), 3.69 (d, 8H, J=14.1 Hz); FAB-MS: *m/z* 987 ($[M+^{107}Ag_2+BF_4]^+$, 2.8%), 989 ($[M+^{107}Ag+^{109}Ag+BF_4]^+$, 5.0%), 991 ($[M+^{109}Ag_2+BF_4]^+$, 3.0%), 793 ($[M+^{107}Ag]^+$, 6.9%), ($[M+^{109}Ag]^+$, 4.7%). Anal. calcd for $C_{42}H_{42}N_{10}B_2F_8\cdot H_2O$: C, 46.10; H, 4.05; N, 12.80. Found: C, 46.12; H, 4.00; N, 12.83%.

4.2.4. $NH_4^+\subset$1·Pic$^-$. To a solution of $K^+\subset$**1**·Br$^-$ (50.0 mg, 6.0×10^{-2} mmol) in 6 mL of mixed solvent

($CH_2Cl_2-CH_3OH=1/1$) was added an excess of NH_4Pic and the mixture stirred at room temperature overnight. The mixture was filtered, and the solid product rinsed with water and dried. The resultant yellow powder was recrystallized from $CH_2Cl_2-CH_3CN$. Yellow prisms (57.6 mg, quant.). Characterization was done as the Br^- form after anion exchange. $NH_4^+\subset\mathbf{1}\cdot Br^-$: Colorless granules. Mp >241°C (dec. Ar sealed tube); ^1H NMR ($CDCl_3$): δ 8.40 (t, 4H, J=54 Hz, NH_4^+), 7.60 (t, 6H, J=8 Hz, Ar-H), 7.17 (d, 12H, J=8 Hz, Ar-H), 3.60 (s, 24H, $-CH_2$-); FAB-MS: *m/z* 704 (M^+). Anal. calcd for $C_{42}H_{46}N_{11}Br$: C, 64.28; H, 5.91; N, 19.63. Found: C, 64.19; H, 5.86; N, 19.39%.

4.3. Crystal data

4.3.1. $2Ag^+\subset\mathbf{2}\cdot 2BF_4^-\cdot H_2O$. $C_{45}H_{42}N_{10}O_3B_2F_8Ag_2$, M_r=1160.24 g mo1^{-1}, colorless prism (grown from MeOH), size 0.50×0.15×0.10 mm^3, triclinic, space group $P\bar{1}$(#2), a=13.5492(5) Å, b=16.9215(5) Å, c=11.9515(5) Å, α=105.309(2)°, β=114.69765(8)°, γ=95.2771(8)°, V=2336.3(2) Å^3, Z=2, ρ_{calcd}=1.649 g cm^{-3}, μ(Mo Kα)=9.21 cm^{-1}, F(000)=1164.00, T=−180±1°C using the $\omega-2\theta$ scan technique to a maximum 2θ value of 55.0°. A total of 21847 reflections were collected. The final cycle of the full-matrix least-squares refinement was based on 9341 observed reflections ($I>3.00\sigma(I)$) and 703 variable parameters and converged with unweighted and weighted agreement factors of R=0.035, Rw=0.068, and GOF=1.19. The maximum and minimum peaks on the final difference Fourier map corresponded to 1.00 and −0.78 e$^-$ Å^{-3}, respectively.

4.3.2. $NH_4^+\subset\mathbf{1}\cdot Pic^-$. $C_{48}H_{48}N_{14}O_7$, M_r=933.00 g mol^{-1}, yellow prism (grown from $CH_2Cl_2-CH_3CN$ mixture), size 0.50×0.40×0.30 mm^3, monoclinic, space group $P1$(#4), a=10.644(2) Å, b=16.885(6) Å, c=13.063(3) Å, β=100.08(1)°, V=2311.5(9) Å^3, Z=2, ρ_{calcd}=1.340 g cm^{-3}, μ(Mo Kα)=0.94 cm^{-1}, F(000)=980.00, T=−150±1°C using the $\omega-2\theta$ scan technique to a maximum 2θ value of 55.0°. A total of 4817 reflections were collected. The final cycle of the full-matrix least-squares refinement was based on 4211 observed reflections ($I>3.00\sigma(I)$) and 670 variable parameters and converged with unweighted and weighted agreement factors of R=0.106, Rw=0.099, and GOF=3.10. The maximum and minimum peaks on the final difference Fourier map corresponded to 1.08 and −0.72 e$^-$ Å^{-3}, respectively.

Crystallographic data (excluding structure factors) for the structures in this paper have been deposited with the Cambridge Crystallographic Data Centre as supplementary publication numbers CCDC 111964 for $NH_4^+\subset\mathbf{1}\cdot Pic^-$ and CCDC 191527 for $2Ag^+\subset\mathbf{2}\cdot 2BF_4^-\cdot H_2O$. Copies of the data can be obtained, free of charge, on application to CCDC, 12 Union Road, Cambridge CB2 1EZ, UK. (fax: +44-(0)1223 336033 or e-mail: deposit@ccdc.cam.ac.uk).

References

1. (a) Takemura, H.; Shinmyozu, T.; Inazu, T. *Tetrahedron Lett.* **1988**, *29*, 1789–1792. (b) Takemura, H.; Shinmyozu, T.; Inazu, T. *J. Am. Chem. Soc.* **1991**, *113*, 1323–1331. (c) Takemura, H.; Shinmyozu, T.; Inazu, T. *Coord. Chem. Rev.* **1996**, *156*, 183–200. (d) Takemura, H.; Inazu, T. *J. Synth. Org. Chem. Jpn.* **1998**, *56*, 604–614. (e) Kon, N.; Takemura, H.; Otsuka, K.; Tanoue, K.; Nakashima, S.; Yasutake, M.; Tani, K.; Kimoto, J.; Shinmyozu, T.; Inazu, T. *J. Org. Chem.* **2000**, *65*, 3708–3715.
2. Takemura, H.; Osada, S.; Shinmyozu, T.; Inazu, T. *J. Chem. Soc., Perkin Trans. 1* **1996**, 277–280.
3. Alpha, B.; Anklam, E.; Deschenaux, R.; Lehn, J.-M.; Pietraszkiewicz, M. *Helv. Chim. Acta* **1988**, *71*, 1042–1052.
4. Because compound **2** absorbs water molecules and causes the broadening and shifting of the signals in ^1H NMR, it was dried in vacuum at 100°C prior to use.
5. Matsuura, N.; Umemoto, K.; Takeda, Y.; Sasaki, A. *Bull. Chem. Soc. Jpn.* **1976**, *49*, 1246–1249.
6. The compositions of alkali metal complexes were determined by the proton ratio of the picrate anion and the ligand after isolation of the complexes.
7. Takemura, H.; Kon, N.; Tani, K.; Takehara, K.; Kimoto, J.; Shinmyozu, T.; Inazu, T. *J. Chem. Soc., Perkin Trans. 1* **1997**, 239–246.
8. (a) Baes, C. F.; Mesmer, R. E. *The Hydrolysis of Cations*. Wiley-Interscience: New York, 1976. (b) Barnum, D. W. *Inorg. Chem.* **1983**, *22*, 2297–2305.
9. Takemura, H.; Nakashima, S.; Kon, N.; Yasutake, M.; Shinmyozu, T.; Inazu, T. *J. Am. Chem. Soc.* **2001**, *123*, 9293–9298.
10. (a) Kelm, H.; Krüger, H.-J. *Eur. J. Inorg. Chem.* **1998**, 1381–1385. (b) Koch, W. O.; Kaiser, J. T.; Krüger, H.-J. *Chem. Commun.* **1997**, 2237–2238.
11. Izutsu, K. *Acid–Base Dissociation Constants in Dipolar Aprotic Solvents. IUPAC Chemical Data Series No. 35*, Blackwell: Oxford, 1990.
12. Sheldrick, G. M. *A Program for the Solution of Crystal Structures*; University of Goettingen: Germany, 1997.
13. Altomare, A.; Burla, M. C.; Camalli, M.; Cascarano, M.; Giacovazzo, C.; Guagliardi, A.; Polidori, G. *J. Appl. Cryst.* **1994**, *27*, 435.
14. DIRDIF 94: Beurskens, P. T.; Admiraal, G.; Beurskens, G.; Bosman, W. P.; de Gelder, R.; Israel, R.; Smits, J. M. M. The DIRDIF-94 program system, Technical Report of the Crystallography Laboratory, University of Nijmegen, The Netherlands, 1994.